Agricultural and Forest Meteorology 295 (2020) 108189

Contents lists available at ScienceDirect

Agricultural and Forest Meteorology

journal homepage: www.elsevier.com/locate/agrformet

Carbon dioxide balance of an oil palm plantation established on tropical peat

Frankie Kiew[a,b], Ryuichi Hirata[c], Takashi Hirano[d,*], Wong Guan Xhuan[a,b], Edward Baran Aries[a], Kevin Kemudang[a], Joseph Wenceslaus[a], Lo Kim San[a], Lulie Melling[a]

[a] Sarawak Tropical Peat Research Institute, Lot 6035, Kuching-Kota Samarahan Expressway, 94300 Kota Samarahan, Sarawak, Malaysia
[b] Graduate School of Agriculture, Hokkaido University, Sapporo, 060-8589, Japan
[c] National Institute for Environmental Studies, Tsukuba 305-8506, Japan
[d] Research Faculty of Agriculture, Hokkaido University, Sapporo, 060-8589, Japan

ARTICLE INFO

Keywords:
CO_2 flux
Decomposition
Drainage
Eddy covariance technique
Mortality
Woody debris

ABSTRACT

Oil palm plantations have been expanding in recent decades in Indonesia and Malaysia. Carbon-rich tropical peat swamp forest has not been excluded from this expansion, because it was the last frontier suitable for industrial agriculture and more accessible than other undeveloped areas. Carbon dioxide (CO_2) emission through accelerated peat decomposition is one of the main environmental concerns in the conversion of peatlands into plantations, which undergo drainage to increase palm growth rates and production. Changes in aboveground biomass might also significantly alter the CO_2 exchange dynamics of the ecosystem. Despite the potential changes in CO_2 balance due to land conversion, so far no study has been conducted using the eddy covariance technique about the CO_2 balance of oil palm plantations established on peat. We have monitored the eddy CO_2 flux above an oil palm plantation on peat in Sarawak, Malaysia since 2011. During the period from 2011 to 2014 (four years), the plantation at 7–10 years of age was a large stable CO_2 source with an annual net ecosystem CO_2 exchange (NEE) of 994 ± 158 g C m^{-2} yr^{-1}. The NEE was much more positive than that of a peat swamp forest (-136 ± 51 g C m^{-2} yr^{-1}) in the same region during the same period. The large positive NEE was caused mainly by its relatively small gross primary production (GPP) (2529 ± 125 g C m^{-2} yr^{-1}) due to low leaf area index resulting from high palm mortality. In addition, a large amount of plant debris left in the plantation probably contributed to the large NEE through decomposition, especially under the many canopy gaps due to high palm mortality mainly caused by toppling on poorly compacted peat. Adequate peat compaction is essential to reduce the mortality rate.

1. Introduction

Peat is a carbon-rich material consisting of dead plant matter, which has accumulated under water-saturated conditions. It is mainly distributed in northern high latitudes where cool climate slows the decomposition of organic matter, but peat has also formed widely in the tropics under water-saturated conditions with slow decomposition rates. Tropical peat is concentrated in insular Southeast Asia, the Congo Basin and the upper Amazon (Page et al., 2011). The total area of tropical peatland, including the newly found huge area in the Congo Basin, is estimated at 5.8 × 10^5 km^2 (Dargie et al., 2017; Page et al., 2011). This latest finding increased the known carbon stock in tropical peat to 105 Pg, accounting for 17% of global peat carbon (Dargie et al., 2017; Page et al., 2011). In Southeast Asia, mainly in Indonesia and Malaysia, peat occupies 2.5 × 10^5 km^2 (Page et al., 2011).

Tropical peat is primarily composed of woody materials which have accumulated over millennia in coexistence with swamp forest in Southeast Asia (Dommain et al., 2011). However, since the 1970s part of the swamp forest has been deforested and converted into smallholders' and industrial plantations, mainly for oil palm and pulpwood trees. Land-use change accelerated from the mid-1980s (Miettinen et al., 2012). In Peninsular Malaysia, Sumatra and Borneo, 7.3 × 10^4 km^2 of peat swamp forest was lost during the 25 years from 1999, while industrial oil palm plantations on peatland had expanded up to 3.1 × 10^4 km^2 by 2015 (Miettinen et al., 2016). Oil palm (*Elaeis guineensis* Jacq) is a highly profitable cash crop and an economically efficient oil crop because of its easy establishment, low maintenance costs and high yield (Dislich et al., 2017). Palm oil is the vegetable oil

* Corresponding author.
E-mail address: hirano@env.agr.hokudai.ac.jp (T. Hirano).

https://doi.org/10.1016/j.agrformet.2020.108189
Received 5 June 2020; Received in revised form 3 September 2020; Accepted 5 September 2020

with the greatest production in the world, and about 85% is produced by Indonesia and Malaysia. Global demand is expected to double by 2030 from that in 2000 (Yan, 2017). Thus, the oil palm plantations will tend to expand to meet the growing global demand.

The conversion of tropical forest to oil palm plantations changes the ecosystem functions, leading to losses of biodiversity, carbon stock and evapotranspiration (Dislich et al., 2017). Temporary huge carbon losses occur owing to deforestation and land clearing using fire (Kotowska et al., 2015; Murdiyarso and Adiningsih, 2007), but soil organic matter and woody debris continue to be decomposed over decades (Guillaume et al., 2018). To develop oil palm plantations, peatlands are drained to lower groundwater level (GWL) to keep productivity high. The lowered GWL enhances oxidative peat decomposition and potentially makes the plantation a large carbon dioxide (CO_2) source. Murdiyarso et al. (2010) estimated the annual net CO_2 emissions from oil palm plantations to be 16.2 Mg C ha^{-1} yr^{-1} over 25 years using the 'gain-loss' and 'stock-difference' methods, of which 38% and 62% arose from biomass loss and peat loss, respectively. Miettinen et al. (2017) assessed peat oxidation in insular Southeast Asia using satellite images and IPCC-based emission factors. They reported that CO_2 emissions amounted to 49 and 64 Tg C yr^{-1}, respectively, from smallholders' and industrial plantations in 2015, which together accounted for 78% of the total peat oxidation in the region. These studies indicate that oil palm plantations established on peat constantly emit a large amount of CO_2 mainly because of peat decomposition. On the other hand, deforestation generally increases albedo (Betts, 2000), which decreases the absorption of shortwave radiation. Also, lowering GWL is expected to decrease methane (CH_4) emissions (Hirano et al., 2009; Melling et al., 2005a; Sakabe et al., 2018; Wong et al., 2020). In order to quantify how much CO_2 is emitted from oil palm plantations, it is essential to directly measure CO_2 balance in the field. To our knowledge, however, there is still no study reporting the ecosystem-scale CO_2 balance of oil palm plantations on tropical peat based on long-term eddy flux data, whereas several studies investigated soil CO_2 efflux using the chamber method (e.g. Dariah et al., 2014; Ishikura et al., 2018; Melling et al., 2013). A recently published paper on eddy CO_2 flux on mineral soil (Meijide et al., 2020) reported that annual net ecosystem CO_2 exchange (NEE) was 1012 and −754 g C m^{-2} yr^{-1}, respectively, in young (1-year-old) and mature (12–13-year-old) plantations in Sumatra, Indonesia. The considerable difference between these two NEE values suggests that the NEE of oil palm plantations changes drastically from being a large CO_2 source to a large sink with advancing age.

We measured CO_2 flux by the eddy covariance technique above an oil palm plantation (OPP) established on peat in Sarawak, Malaysia for four years starting in 2011. The objectives of this study were to (1) quantify NEE, gross primary production (GPP) and ecosystem respiration (RE); (2) examine how environmental factors influence the CO_2 fluxes; and (3) discuss the paths of CO_2 flow in the plantation and the effect of land conversion on the CO_2 balance through comparison with CO_2 fluxes measured in a peat swamp forest (PSF) in the same region during the same period (Kiew et al., 2018). This study can contribute to evaluating the effect of conversion of tropical peatlands on CO_2 balance.

2. Material and methods

2.1. Study site

The study was conducted in an oil palm plantation (OPP; 2°11′N, 111°50′E) established on coastal peat (Dommain et al., 2011) in Sibu, Sarawak, Malaysia. The landscape was flat and horizontal, and thus suitable for eddy flux measurement. Mean annual temperature and precipitation were 26.5 ± 0.2 °C and 2915 ± 213 mm yr^{-1} (mean ± 1 standard deviation (SD)), respectively, between 2004 and 2016 at the Sungai Salim B meteorological station 7.4 km away from the study site. A mixed peat swamp forest with an area of about 100 km^2 and peat depth of about 13 m was converted to a plantation in 2004.

2.2. Oil palm establishment

The site was clear-cut, and tree biomass was partially burnt on site to improve access and workability. The lightly burned remains of stems, branches and stumps were stacked on the ground in rows (stacking rows). Ditches were dug to a depth of −1.0 – −1.7 m, and water gates were built to control groundwater level (GWL) at an annual average of −0.6 m. Then the peat was compacted to increase soil bulk density in order to reduce leaning and toppling of palms and increase soil moisture holding capacity. Palm seedlings were planted in September 2004 in a regular triangular pattern with 8.5 m spacing, resulting in a density of 153 palms ha^{-1}.

By 2014, 43% of the palms had died because of toppling and disease, which decreased the palm density to 87 palms ha^{-1} with many canopy gaps. In addition, some palms were leaning badly but still alive. The low palm density resulted from insufficient peat compaction before planting. When the plantation was established, the importance of compaction was not well understood. The canopy height was about 8 m in 2014. Plant area index (PAI) measured with a plant canopy analyzer (LAI2200; LI-COR Inc., Lincoln, NB, USA) averaged at 3.7 m^2 m^{-2} between 2013 and 2014, which was 20% lower than that of an adjacent 3.5-year-younger plantation. The ground was sparsely covered with fern plants (*Stenochlaena palustris*). Little litter accumulated on the ground except for in fern-covered areas. Each month one or two fronds were pruned from each palm and stacked in inter-row spaces to recycle nutrients and build-up soil organic matter. Similarly, empty fresh bunches (EFB) were returned to the plantation. Urea (74–147 kg N ha^{-1} yr^{-1}), rock phosphate (7–9 kg P ha^{-1} yr^{-1}) and muriate of potash (239–311 kg K ha^{-1} yr^{-1}) were applied together four times a year within 1 m from each stem. Further information on fertilization is provided by (Ishikura et al., 2018).

2.3. Measurement of flux and environmental factors

A 40-m-tall tower was built in 2010 at the OPP. CO_2 flux has been continuously measured since January 2011 at a height of 21 m on the tower by the eddy covariance technique with a sonic anemometer-thermometer (CSAT3; Campbell Scientific Inc., Logan, UT, USA) and an open-path CO_2/H_2O analyzer (LI7500A; LI-COR Inc.). The flux sensors are separated by 0.2 m. Sensor signals are recorded with a datalogger (CR3000; Campbell Scientific Inc.) at 10 Hz. CO_2 concentrations are also measured every minute with a closed-path CO_2 analyzer (LI820; LI-COR Inc.) at six heights of 0.5, 1, 3, 5, 11 and 21 m. The sampling lines are changed every minute in rotation. Both open-path and closed-path analyzers are calibrated monthly using standard gasses. In addition, four components of radiation are measured with a radiometer (CNR4; Kipp & Zonen, Delft, the Netherlands) at the tower top. Downward and upward photosynthetic photon flux densities (PPFDs) are also measured with quantum sensors (LI-190; LI-COR Inc.) at the same height. Air temperature and relative humidity are measured at 21 m with a temperature/humidity probe (CS215; Campbell Scientific Inc.) in a radiation shield (41,303–5A; Campbell Scientific Inc.). These meteorological variables are measured every 10 s, and their 5 min means are recorded with the above datalogger.

The GWL, a distance between ground and water surfaces, is measured half-hourly with a water level logger (STS DN/L 50; Sensor Technik Sirnack AG, Danbury, CT, USA). Volumetric soil water content (SWC) is measured in the uppermost 30-cm-thick layer with a TDR sensor (CS615; Campbell Scientific Inc.). GWL and SWC are measured at a single point, because the ground is almost level after compaction. Thus, their spatial variations might be small. Precipitation is measured with a tipping-bucket rain gage (TE525; Campbell Scientific Inc.) at the

height of 1 m at the center of a large canopy gap with a radius of 2–3 m. These sensors were installed within 10 m from the tower. All these environmental factors have also been continuously measured since January 2011.

2.4. Flux calculation, quality control, gap filling and partitioning

Half-hourly mean eddy CO_2 flux was calculated from raw data for four years from 2011 through 2014 using Flux Calculator software (Ueyama et al., 2012). Spike removal (Vickers and Mahrt, 1997), planar fit rotation (Wilczak et al., 2001), frequency response correction (Massman, 2000) and air density fluctuation correction (Webb et al., 1980) were applied. CO_2 storage change in airspace below the eddy sensors was estimated from the temporal change of CO_2 profiles measured at six heights (Hirano et al., 2007). Then net ecosystem CO_2 exchange (NEE) was calculated as the sum of the eddy CO_2 flux and CO_2 storage change.

Quality control and gap filling were conducted with the same method as in Kiew et al. (2018). Firstly, if NEE was beyond 3 SDs from mean diurnal variation calculated using a 13-day-long moving window, the NEE was removed as an outlier (Papale et al., 2006). Secondly, nighttime NEE (PPFD $\leq$ 10 μmol m^{-2} s^{-1}) was screened using a friction velocity (u^*) threshold of 0.21 m s^{-1}, which was determined using Flux Analysis Tool software (Ueyama et al., 2012). As a result, 75% of half-hourly NEE was totally lost in the four years, including system malfunctions mainly due to power problems. Finally, the data gaps were filled by the marginal distribution sampling (MDS) method (Reichstein et al., 2005) separately for the daytime (PPFD > 10 μmol m^{-2} s^{-1}) and nighttime. The size of moving windows ranged from 7 to 49 days, depending on gap length. Air temperature, PPFD and vapor pressure deficit (VPD) were used for the daytime, whereas air temperature, GWL and SWC for the nighttime. Further information on gap filling was provided by Kiew et al. (2018). Daytime ecosystem respiration (RE) was 'looked up' from nighttime NEE using the same algorithm as for gap filling (MDS), and then gross primary production (GPP) was calculated as the difference between NEE and daytime RE (GPP = RE – NEE). During the nighttime, GPP was set as zero.

Energy balance closure was evaluated as the ratio of eddy energy flux (the sum of sensible and latent heat fluxes) and net radiation, because soil heat flux was not measured. As a result, the ratio was 0.89 on average.

2.5. Data analysis

The responses of half-hourly NEE to environmental factors were analyzed by linear or non-linear regression using R version 3.5.1. For environmental factors, linear regression analysis was also applied using R version 3.5.1. To draw the light curve of daytime NEE, the following nonrectangular hyperbola (Thornley, 1976) was fitted.

$$\mathrm{NEE} = \frac{-\alpha\cdot\mathrm{PPFD} - \mathrm{GPP_{max}} + \sqrt{(\alpha\cdot\mathrm{PPFD} + \mathrm{GPP_{max}})^2 - 4\cdot\alpha\cdot\mathrm{PPFD}\cdot\theta\cdot\mathrm{GPP_{max}}}}{2\cdot\theta} + R_d \quad (1)$$

where α is the initial slope, GPP_{max} maximal GPP, θ curvature and R_d intercept or daytime RE, which are fitting parameters. To illustrate the characteristics of the CO_2 exchange of OPP, we used flux data measured above a secondary peat swamp forest (PSF) in the same region during the same period (Kiew et al., 2018) and compared them between the two sites. PSF lies about 110 km to the south of OPP. PSF's canopy height, plant density, plant area index and peat depth were 25 m, 1990 trees ha^{-1}, 7.9 m^2 m^{-2} and 10 m, respectively (Kiew et al., 2018). A *t*-test was applied to compare mean values between OPP and PSF using R version 3.5.1.

A path analysis was performed to examine the relative importance of environmental factors to GPP and RE using gap-filled monthly data with *sem* package in R version 3.5.1. Causal relationships among variables were modeled using a general structural equation from precipitation to GPP via PPFD, VPD and SWC or to RE via air temperature, VPD, GWL and SWC. Relative strength of direct effect is expressed as a standardized partial regression coefficient (path coefficient), and total effect equals the sum of direct effect and indirect effect according to the model structure (e.g. Fei et al., 2018; Iwata et al., 2015; Ueyama et al., 2014). The adequacy of the model was judged from a goodness-of-fit index (GFI > 0.9) (Sun et al., 2018). The path analysis was also performed using monthly data measured in PSF.

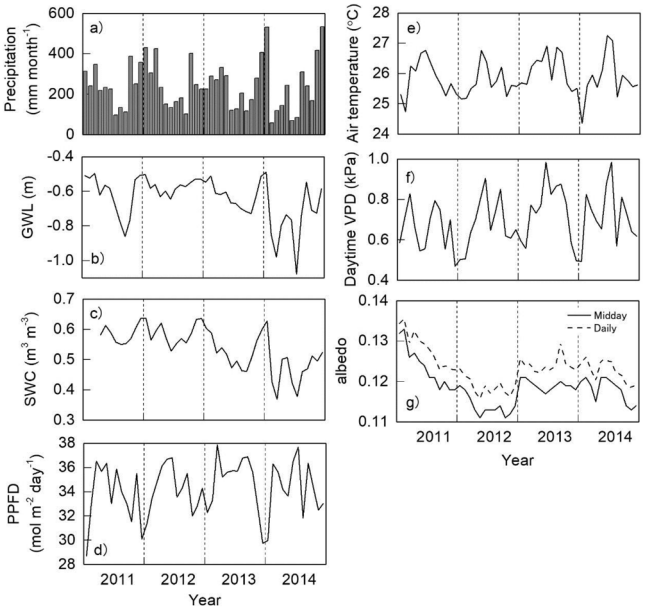

Fig. 1. Temporal variations in monthly values of (a) precipitation, (b) groundwater level (GWL), (c) soil water content (SWC), (d) photosynthetic photon flux density (PPFD), (e) air temperature, (f) daytime (8–16 h) vapor pressure deficit (VPD) and (g) albedo. Albedo was calculated using daily or around-midday (10–14 h) shortwave radiations.

3. Results

3.1. Environmental properties and albedo

Seasonal variation in precipitation was not very distinct (Fig. 1a), though precipitation tended to increase in December and January (Fig. 3). Monthly precipitation had a relatively large variation (242 ± 119 mm $month^{-1}$, mean ± 1 SD) (Fig. 1a); the maxima were recorded at 533 to 535 mm in January and December 2014, whereas the minimum was 34 mm in February 2014. In five months (10.4% of 48 months) precipitation was less than 100 mm, which is a common threshold for tropical dry months (Malhi et al., 2002). Annual precipitation ranged between 2850 and 3015 mm (Table 1), and all values were above the decadal mean (2797 ± 224 mm yr^{-1}) for 2005–2014 at a nearby meteorological station. Monthly mean GWL varied from −1.08 to −0.48 m (Fig. 1b), whereas daily GWL fluctuated between −1.25 and −0.17 m (data not shown). Basically, GWL varied following precipitation (r = 0.53). Less precipitation in the first half of 2014 lowered GWL below −1.0 m in July despite an attempt to control water level with water gates, resulting in an annual mean GWL of −0.75 m in 2014 (Table 1), which was below the targeted GWL of −0.6 m. Monthly mean SWC varied between 0.38 and 0.64 m^3 m^{-3} in parallel with GWL (r = 0.78) (Fig. 1c). Mean monthly PPFD, air temperature and daytime VPD were 34.3 ± 2.2 mol m^{-2} day^{-1}, 25.9 ± 0.6 °C and 0.70 ± 0.13 kPa, respectively (Figs. 1d–f). There was significant positive correlation in each pair of PPFD, air temperature and daytime VPD (p < 0.01). Also, the three factors were each negatively correlated

Table 1
Annual values of CO_2 fluxes and environmental factors. Maximal GPP (GPP_{max}) was determined monthly and averaged.

Year	NEE	RE	GPP	GPP_{max}	GWL	Precipitation	PPFD
	(g C m^{-2} yr^{-1})	(g C m^{-2} yr^{-1})	(g C m^{-2} yr^{-1})	(μmol m^{-2} yr^{-1})	(m)	(mm yr^{-1})	(kmol m^{-2} yr^{-1})
2011	1223	3699	2476	19.5 ± 2.7	−0.62	2850	123
2012	846	3590	2744	20.6 ± 3.3	−0.57	3015	125
2013	1058	3518	2461	21.3 ± 2.5	−0.63	2854	127
2014	849	3285	2436	19.6 ± 2.8	−0.75	2873	125
Mean ± 1 SD	994 ± 158	3523 ± 152	2529 ± 125	20.2 ± 2.9	−0.64 ± 0.07	2898 ± 68	125 ± 1.3

with precipitation ($p < 0.01$). At this site precipitation governed water regime and influenced radiation, air temperature and humidity. Albedo of shortwave radiation showed a decreasing tendency during 2011 and then became nearly stable (Fig. 1g), probably reflecting the expansion of leaf area. Mean values for around-midday (10:00–14:00) and daily albedo were 0.119 ± 0.005 and 0.123 ± 0.004, respectively, which were significantly higher ($p < 0.01$) than those for PSF (0.098 ± 0.003 and 0.101 ± 0.003, respectively).

3.2. Temporal variation in CO_2 flux

Although the diurnal variations of PPFD and VPD were almost the same at the two sites (Figs. 2b–c), NEE was a little higher during the nighttime (18:30–6:00) and less negative during the daytime in OPP than in PSF (Fig. 2a). A little higher VPD in PSF was possibly due to different heights of measurement: 21 m (OPP) vs. 41 m (PSF). Mean NEE in the nighttime were 10.2 (OPP) and 8.6 (PSF) μmol m^{-2} s^{-1}, and negative peaks of NEE were −12.4 μmol m^{-2} s^{-1} at 10:30 (OPP) and −19.9 μmol m^{-2} s^{-1} at 12:00 noon (PSF). The peaking time was 1.5 h ahead in OPP. The mean seasonal variations of gap-filled NEE, GPP and RE were shown in Fig. 3a. No clear seasonal pattern was found in monthly mean NEE, GPP and RE, whereas precipitation and GWL showed an increasing tendency in December and January (Figs. 3b–c).

Annual NEE, GPP and RE of OPP were 994 ± 158, 3523 ± 152 and 2529 ± 125 g C m^{-2} yr^{-1}, respectively, between 2011 and 2014 (Table 1). Over the four years, palms aged from seven to ten years old. Although no data are available on the increase in biomass production at the study site, Khasanah et al., 2015) reported that palm biomass increased linearly over 25 years (a typical replanting cycle). However, no pattern of significant increase was found from 2011 to 2014 in either annual GPP ($r = -0.36$) or annual GPP_{max} ($r = 0.63$) of Eq. (1). In contrast, annual RE was negatively correlated with age ($p < 0.05$).

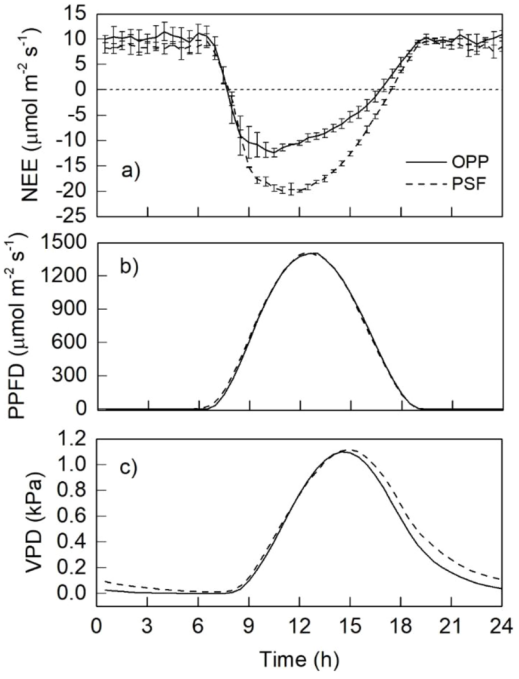

Fig. 2. Mean diurnal variations in (a) NEE, (b) photosynthetic photon flux density (PPFD) and (c) vapor pressure deficit (VPD). Data from both the oil palm plantation (OPP) and the peat swamp forest (PSF) are shown. VPDs were measured at 21 m (OPP) and 41 m (PSF) (Kiew et al., 2018), respectively. Error bars denote 1 standard deviation.

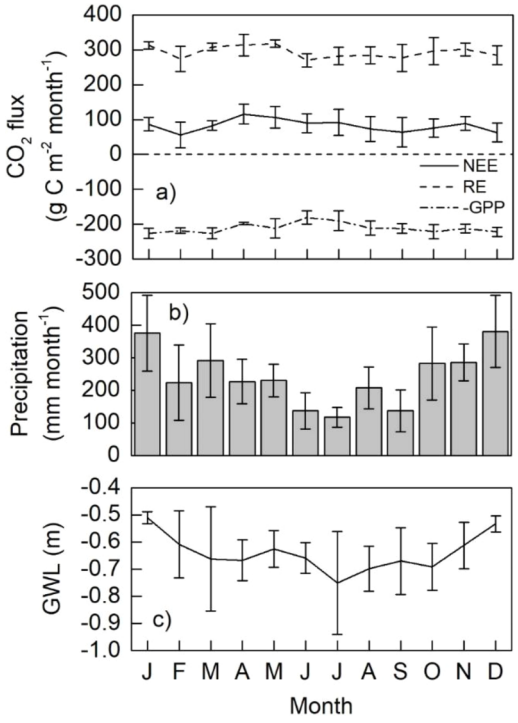

Fig. 3. Mean seasonal variations in monthly values of (a) gap-filled CO_2 fluxes (NEE, RE and GPP), (b) precipitation and (c) groundwater level (GWL). GPP is shown as negative (-GPP). Error bars denote 1 standard deviation.

3.3. Environmental responses of CO_2 flux

The relationship between daytime NEE and PPFD in OPP was approximated using Eq. (1) ($r^2 = 0.40$) with α of 0.0345, GPP_{max} of 18.9 μmol m^{-2} s^{-1}, θ of 0.92 and R_d of 8.6 μmol m^{-2} s^{-1} (Fig. 4). NEE reached saturation at around 1000 μmol m^{-2} s^{-1} in PPFD. To examine the data dispersion from the light-response curve, light-saturated NEE was plotted against VPD (Fig. 5). The light-saturated NEE showed a significant positive relationship ($r = 0.40$) with a slope of 5.56 μmol m^{-2} s^{-1} kPa^{-1}, but VPD explains only 16% ($r^2 = 0.16$) of the dispersion. Differences between measured NEE and predicted NEE from VPD were plotted against GWL or SWC to find other predictors (Fig. 6). Although a significant positive relationship ($p < 0.01$) was found owing to the large number of data points, GWL and SWC, respectively, can explain less than 1% ($r^2 < 0.01$) of the differences.

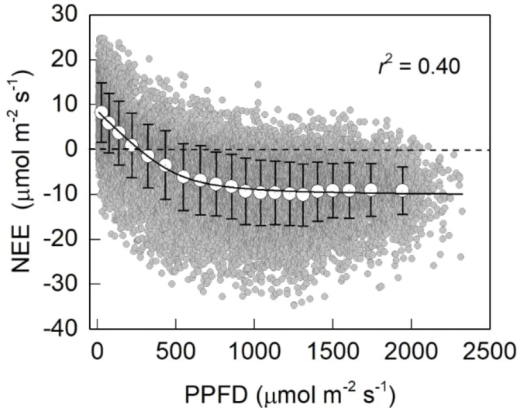

Fig. 4. Relationship between daytime NEE and photosynthetic photon flux density (PPFD). Data were binned equally into 20 classes according to PPFD and averaged. Error bars denote 1 standard deviation. A nonrectangular hyperbola (Eq. (1)) was significantly fitted ($p < 0.001$).

Nighttime NEE, which corresponds to RE, was plotted against GWL or SWC (Fig. 7), because there are a lot of studies reporting that soil CO_2 efflux depended on GWL in various tropical peat ecosystems (e.g. Hirano et al., 2014; Itoh et al., 2017; Wakhid et al., 2017), and soil CO_2 efflux is one of the principal components of RE. However, the relationship with GWL was not significant, whereas that with SWC was significantly positive ($p = 0.0013$) despite a low correlation coefficient ($r = 0.05$).

The path analysis for monthly GPP indicated that the direct effect was strongest in VPD (−0.41), followed by SWC (0.31) and PPFD (0.18) in OPP (Fig. 8a). The path coefficients of VPD and SWC were significant ($p < 0.05$). In contrast, the strongest effect on GPP in PSF was caused by PPFD (0.35), followed by VPD (0.31) and SWC (0.26), although all effects were insignificant (Fig. 8b). The total effects of PPFD on GPP in OPP and PSF including indirect effect via VPD were −0.02 (= 0.49 × (−0.41) + 0.18) and 0.56 (= 0.69 × 0.31 + 0.35), respectively. The direct effect on monthly RE was strongest in SWC (1.03), followed by GWL (−0.74), air temperature (0.27) and VPD (−0.27) in OPP (Fig. 8c). The effects of GWL and SWC on RE were significantly negative and positive in OPP ($p < 0.01$), respectively. In PSF, however, GWL showed the highest coefficient (−0.50), followed by SWC (0.32), VPD (0.32) and air temperature (0.13) (Fig. 8d), though all were insignificant. Although the coefficients of VPD to RE were insignificant, they were negative and positive, respectively, in OPP and PSF.

4. Discussion

The poorly grown oil palm plantation (OPP) with large gaps, in which GWL was controlled, on average, between −0.75 and −0.57 m, was a consistent large CO_2 source over four years when it was 7–10 years old. The annual NEE of OPP was much more positive by 1130 g C m^2 yr^{-1} than that of a secondary peat swamp forest (PSF) in the same region (Kiew et al., 2018) (Fig. 9), where mean GWL was −0.19 ± 0.03 m on an annual basis. The large difference was due to small GPP in OPP despite almost the same RE (Fig. 9). Similarly, the OPP's NEE was more positive by far than those of three peat swamp forests in Central Kalimantan, Indonesia (Hirano et al., 2012); the annual NEE of relatively intact forest, drained forest and burned ex-forest were 174 ± 203, 328 ± 204 and 499 ± 72 g C m^{-2} yr^{-1}, respectively. The OPP's NEE was three times larger than that of the drained forest, though their GWLs were similar (−0.64 ± 0.07 (OPP) vs. −0.55 ± 0.11 m). The large difference in annual NEE between OPP and the drained forest was also attributed to GPP difference. In addition, the OPP's annual NEE of 994 g C m^{-2} yr^{-1} lies at the top of the NEE's ranking from 506 site-years of worldwide data (Baldocchi, 2008) and is about 1400 g C m^{-2} yr^{-1} more positive than mean annual NEE of tropical humid evergreen forests on mineral soil (Luyssaert et al., 2007). In contrast, the NEE of OPP is equivalent to that of a 1-year-old oil palm plantation on mineral soil (1012 g C m^{-2} yr^{-1}) in Sumatra, Indonesia (Meijide et al., 2020). In the same region, however, a 12–13-year-old oil palm plantation on mineral soil was a large CO_2 sink with the annual NEE of −754 g C m^{-2} yr^{-1} (Meijide et al., 2020); GPP and RE are not shown in the paper.

The annual GPP of OPP (2529 g C m^{-2} yr^{-1}) was about 70% of PSF (Kiew et al., 2018) (Fig. 9), other tropical peat swamp forests (Hirano et al., 2012) and tropical humid evergreen forests (Luyssaert et al., 2007). The smaller GPP was attributable to lower plant area index (PAI) due to the low tree density (87 trees ha^{-1}). Although PAI consists not only of leaves but also of stems and branches, the PAI of OPP was less than half that of PSF (Kiew et al., 2018) (3.7 vs. 7.9 m^2 m^{-2}). In addition, OPP's PAI was lower by about 20% than that of an adjacent 3.5-year-younger plantation. On the contrary, Manoli et al. (2018) simulated GPP using an ecohydrological model (Tethys & Chloris) based on field data measured in oil palm plantations on mineral soil (Meijide et al., 2017) and reported that annual GPP exceeded 3000 g C m^{-2} yr^{-1} in five years and became saturated at around 4000 g C m^{-2} yr^{-1} in 6–7 years. According to the simulation for a healthy oil palm plantation, the annual NEE of OPP could be estimated to be about −500 g C m^{-2} yr^{-1}, which indicates a considerable amount of CO_2 uptake but is less negative than −754 g C m^{-2} yr^{-1} of a mature oil palm plantation on mineral soil (Meijide et al., 2020).

The annual RE of OPP (3523 g C m^{-2} yr^{-1}) was almost equivalent to those of peat swamp forests (Hirano et al., 2012; Kiew et al., 2018) (Fig. 9). In OPP, annual total soil respiration and heterotrophic soil respiration excluding root respiration, measured using an automated chamber system without litter accumulation and buried coarse woody debris (Ishikura et al., 2018), were 1030 and 690 g C m^{-2} yr^{-1}, respectively. Thus, the heterotrophic soil respiration corresponds to oxidative peat decomposition. The total soil respiration accounted for about 30% of the RE. Both the total and heterotrophic soil respirations were lower than those of other oil palm plantations on peat, ranging from 1220 to 1810 g C m^{-2} yr^{-1} for total respiration (Dariah et al., 2014; Melling et al., 2005b; Melling et al., 2013; Sakata et al., 2015) and from 690 to 1800 g C m^{-2} yr^{-1} for heterotrophic respiration (Dariah et al., 2014; Husnain et al., 2014; Marwanto and Agus, 2014; Melling et al., 2013). The lower respirations in OPP might be due to higher GWL than those of previous studies. There was a large amount of plant debris both under and above the ground in OPP. Coarse woody roots, including large buttresses, were left underground, as was the common procedure in the early years of tropical peatland preparation. Lightly burned tree stems, branches and stumps were stacked in lines on the ground before oil palm seedlings were planted. In addition, a few dead oil palms were left in the site. It is also a common plantation practice to recycle nutrients by stacking pruned fronds on the ground and returning empty fruit bunches (EFBs) to the plantation by laying them on the ground. The decomposition of all the above-mentioned plant debris contributed to the relatively large RE. Here, we simply estimate the contribution of the plant debris decomposition to RE. The difference (2595 g C m^{-2} yr^{-1}) between RE (3285 g C m^{-2} yr^{-1}) and soil heterotrophic respiration (690 g C m^{-2} yr^{-1}) corresponds to the sum of plant respiration and the decomposition of all the debris. Plant respiration is reported to be about half of GPP (Chapin III et al., 2011). Thus, annual plant respiration could be 1218 g C m^{-2} yr^{-1} (= 2436 / 2), and annual CO_2 emissions through the debris decomposition is estimated to be 1377 g C m^{-2} yr^{-1} (= 2595 - 1218), which is twice as much as for heterotrophic soil respiration or oxidative peat decomposition.

Hardwick et al. (2015) and Meijide et al. (2018) have reported that air temperature, VPD and soil temperature were higher in oil palm

plantations than in primary forests mainly because of lower leaf area index (LAI) in plantations. On our site the low palm density caused by mortality should have changed microclimate especially under canopy gaps. Temperatures of soil, air and coarse woody debris (CWD) rose in canopy gaps, because more solar radiation reached the ground (Forrester et al., 2012; Muscolo et al., 2014), and soil water content was increased by reduced transpiration (Denslow, 1987). The higher temperature and soil water content probably enhanced the decomposition of surface peat and buried CWD in this site. Alternatively, aboveground CWD was dried by increased evaporation due to higher air temperature and increased solar radiation in gap openings (Forrester et al., 2012). The decomposition of CWD is enhanced by higher temperature but potentially suppressed by lower water content. Forrester et al. (2015) reported that CO_2 efflux through CWD decomposition increased immediately after gap opening in comparison with under the closed canopy, but the significant increase ceased within four years, which suggests a tradeoff between the two opposite effects on decomposition.

The results of path analysis (Fig. 8) show that GPP responded to VPD negatively and to SWC positively in OPP on a monthly basis, supporting the knowledge that oil palms are sensitive to water deficit (Dislich et al., 2017; Manoli et al., 2018). A negative relationship was also found between light-saturated NEE and VPD on a half-hourly basis (Fig. 5), though VPD accounted for only 16% of the variation of light-saturated NEE. In addition, residuals between measured NEE and predicted NEE from VPD were almost independent of GWL and SWC ($r^2 < 0.01$) (Fig. 6), suggesting that the response of photosynthesis to VPD was not sensitive to groundwater regime on a half-hourly basis.

The effects of GWL and SWC on RE were negative and positive, respectively, in both sites. In addition, GWL and SWC were positively correlated. GWL lowering enhanced oxidative peat decomposition, whereas its resultant decreased SWC probably depressed the decomposition of dead organic matter such as buried dead roots and EFBs left under and on the ground because of desiccation (Hirano et al., 2014). SWC should have reflected the water content of the dead matter. The path coefficient of SWC to RE was much higher in OPP, suggesting that RE was more sensitive to SWC in OPP than in PSF. The higher sensitivity in OPP was probably because OPP had more CWD and was in drier conditions due to drainage and the sparser canopy. In PSF the ground surface was usually wet. A positive relationship between RE and SWC was also found in half-hourly RE (Fig. 7). The effect of VPD on RE was negative in OPP although not significant. VPD would have reflected the water content of aboveground plant debris in stacking rows and frond piles, which were not touching the soil surface. Thus, high VPD enhanced debris desiccation and probably decreased its decomposition.

The albedo of OPP was 0.119 ± 0.005 around midday (Fig. 1) and significantly lower by 0.02 than that of PSF (Kiew et al., 2018), which

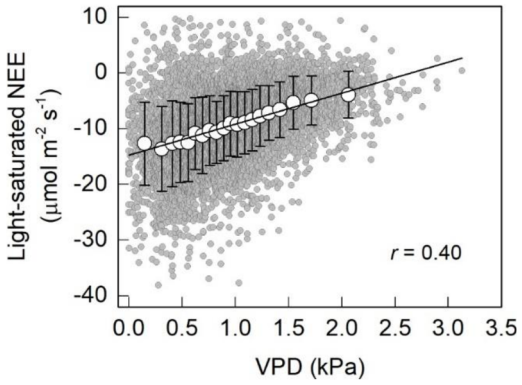

Fig. 5. Relationship between light-saturated NEE (PPFD > 1000 μmol m^{-2} s^{-1}) and vapor pressure deficit (VPD). Data were binned equally into 20 classes according to VPD and averaged. Error bars denote 1 standard deviation. A regression line was significantly drawn ($p < 0.001$).

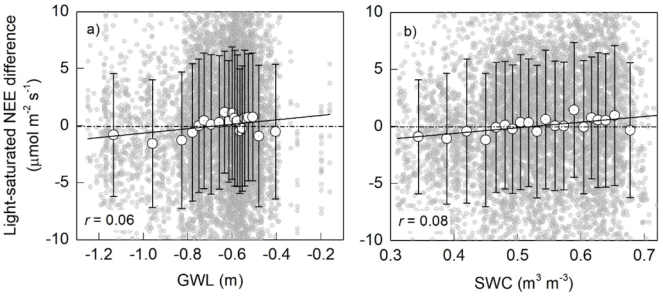

Fig. 6. Relationship of the difference between measured and predicted light-saturated NEE (PPFD > 1000 μmol m^{-2} s^{-1}) with (a) groundwater level (GWL) and (b) soil water content (SWC). Light-saturated NEE was predicted from vapor pressure deficit (VPD) using the regression line in Fig. 5. The NEE difference was calculated as "measured" minus "predicted". Data were binned equally into 20 classes according to GWL or SWC and averaged. Error bars denote 1 standard deviation. A significant trend was found in both panels ($p < 0.01$).

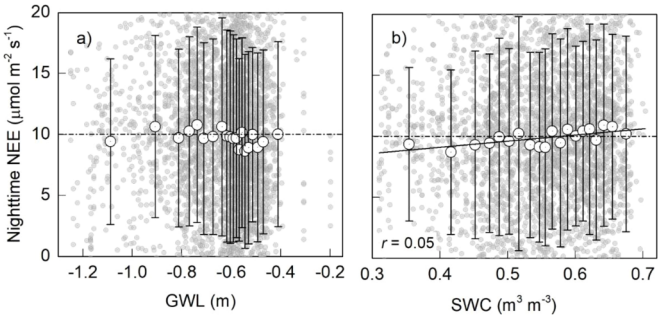

Fig. 7. Relationship between nighttime NEE and (a) groundwater level (GWL) and (b) soil water content (SWC). Data were binned equally into 20 classes according to GWL or SWC and averaged. Error bars denote 1 standard deviation. A significant trend was found only in panel b ($p = 0.0013$).

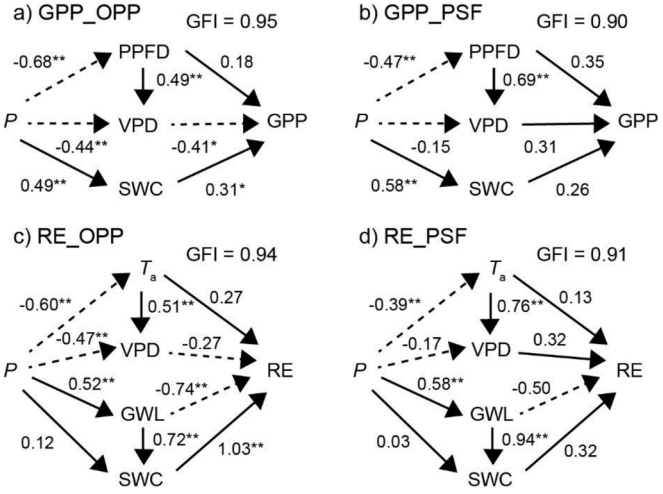

Fig. 8. Path diagrams of GPP and RE using monthly data for the oil palm plantation (OPP) and the peat swamp forest (PSF). P is precipitation, T_a air temperature, VPD vapor pressure deficit, SWC soil water content and GWL groundwater level. GFI stands for a goodness-of-fit index. Solid and broken lines denote positive and negative effects, respectively. The significant level of path coefficients is denoted by * ($p < 0.05$) or ** ($p < 0.01$).

decreased absorbed shortwave radiation. The OPP's albedo was lower than that (0.14 ± 0.01) of a 12-year-old oil palm plantation on mineral soil (Meijide et al., 2017). The difference in albedo between the two plantations was partly due to different soil types. In addition, CH_4

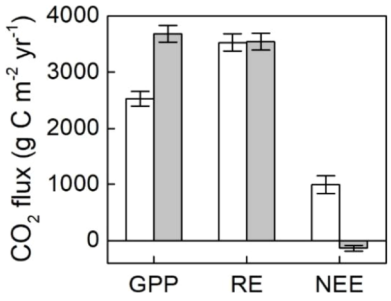

Fig. 9. Comparison of annual GPP, RE and NEE from 2011 to 2014 between the oil palm plantation (OPP, white) and the peat swamp forest (PSF, gray; (Kiew et al., 2018)). Vertical bars denote 1 standard deviation.

emission was less in OPP (2.19 ± 0.21 g C m^{-2} yr^{-1}) than in PSF (4.17 ± 0.69 g C m^{-2} yr^{-1}) mainly because of lowered GWL (Wong et al., 2020). The difference in annual CH_4 emissions (−1.98 g C−CH_4 m^{-2} yr^{-1}) can be converted into −20 g C−CO_2 m^{-2} yr^{-1} using a global warming potential (GWP) factor of 28 over a timescale of 100 years (IPCC, 2013). The decreased CH_4 emission was too small to compensate for the large difference in NEE (1130 g C m^{-2} yr^{-1}) between PSF and OPP.

5. Conclusions

Eddy CO_2 flux was measured for four years above an oil palm plantation established on tropical peat, which was converted from a peat swamp forest. In comparison with a peat swamp forest, the plantation showed less GPP by about 30% and almost the same RE, which resulted in an annual NEE of 994 g C m^{-2} yr^{-1} on average in the plantation. The large positive NEE was caused by less GPP due to low palm density. The palm density of the plantation was only 87 palms ha^{-1}. The 43% of planted palms died in 10 years mainly because of toppling. The serious toppling resulted from insufficient peat compaction during land preparation. Although peat compaction is an essential procedure to develop plantations on peat, the importance of compaction was not well understood in 2004 when the plantation was established. In addition, a large amount of plant debris left in the plantation probably contributed to the large NEE through decomposition especially under many canopy gaps due to low palm density.

Further field studies on eddy CO_2 flux are necessary in healthy oil palm plantations established on adequately compacted peat. Moreover, studies in young plantations on peat are important, because a young oil palm plantation showed a large positive annual NEE of 1012 g C m^{-2} yr^{-1} even on mineral soil (Meijide et al., 2020). It is expected that more CO_2 is emitted from young plantations on peat.

Declaration of Competing Interest

The authors declare that they have no known competing financial interests or personal relationships that could have appeared to influence the work reported in this paper.

The authors declare the following financial interests/personal relationships which may be considered as potential competing interests:

Acknowledgements

This work was supported by both the Sarawak State Government and the Federal Government of Malaysia, and was partly supported by the Environmental Research and Technology Development Fund (grant number 2-1504) of the Environmental Restoration and Conservation Agency, Japan and JSPS KAKENHI Grant Number JP19H05666. We are thankful to all the staff members of Sarawak Tropical Peat Research Institute for all their assistance especially in the maintenance of the flux measurements at the tower. We would also like to thank Goh Kah Joo for his invaluable comments on the manuscript.

References

Baldocchi, D., 2008. 'Breathing' of the terrestrial biosphere: lessons learned from a global network of carbon dioxide flux measurement systems. Aust. J. Bot. 56 (1), 1–26.
Betts, R., 2000. Offset of the potential carbon sink from boreal forestation by decreases in surface albedo. Nature 408, 187–190.
Chapin III, F.S., Matson, P.A, Vitousek, P.M., 2011. Principles of Terrestrial Ecosystem Ecology. Springer, pp. 529 pp.
Dargie, G.C., Lewis, S.L., Lawson, I.T., Mitchard, E.T.A., Page, S.E., Bocko, Y.E., Ifo, S.A., 2017. Age, extent and carbon storage of the central Congo Basin peatland complex. Nature 542 (7639), 86–90.
Dariah, A., Marwanto, S., Agus, F., 2014. Root- and peat-based CO_2 emissions from oil palm plantations. Mitig. Adapt. Strateg. Glob. Change 19 (6), 831–843.
Denslow, J.S., 1987. Tropical rainforest gaps and tree species diversity. Annu. Rev. Ecol. Syst. 18, 431–451.
Dislich, C., Keyel, A.C., Salecker, J., Kisel, Y., Meyer, K.M., Auliya, M., Barnes, A.D., Corre, M.D., Darras, K., Faust, H., Hess, B., Klasen, S., Knohl, A., Kreft, H., Meijide, A., Nurdiansyah, F., Otten, F., Pe'er, G., Steinebach, S., Tarigan, S., Tölle, M.H., Tscharntke, T., Wiegand, K., 2017. A review of the ecosystem functions in oil palm plantations, using forests as a reference system. Biol. Rev. 92 (3), 1539–1569.
Dommain, R., Couwenberg, J., Joosten, H., 2011. Development and carbon sequestration of tropical peat domes in south-east Asia: links to post-glacial sea-level changes and Holocene climate variability. Quat. Sci. Rev. 30 (7–8), 999–1010.
Fei, X., Song, Q., Zhang, Y., Liu, Y., Sha, L., Yu, G., Zhang, L., Duan, C., Deng, Y., Wu, C., Lu, Z., Luo, K., Chen, A., Xu, K., Liu, W., Huang, H., Jin, Y., Zhou, R., Li, J., Lin, Y., Zhou, L., Fu, Y., Bai, X., Tang, X., Gao, J., Zhou, W., Grace, J., 2018. Carbon exchanges and their responses to temperature and precipitation in forest ecosystems in Yunnan, Southwest China. Sci. Total Environ. 616-617, 824–840.
Forrester, J.A., Mladenoff, D.J., D'Amato, A.W., Fraver, S., Lindner, D.L., Brazee, N.J., Clayton, M.K., Gower, S.T., 2015. Temporal trends and sources of variation in carbon flux from coarse woody debris in experimental forest canopy openings. Oecologia 179 (3), 889–900.
Forrester, J.A., Mladenoff, D.J., Gower, S.T., Stoffel, J.L., 2012. Interactions of temperature and moisture with respiration from coarse woody debris in experimental forest canopy gaps. For. Ecol. Manage. 265, 124–132.
Guillaume, T., Kotowska, M.M., Hertel, D., Knohl, A., Krashevska, V., Murtilaksono, K., Scheu, S., Kuzyakov, Y., 2018. Carbon costs and benefits of Indonesian rainforest conversion to plantations. Nat. Commun. 9 (1), 2388.
Hardwick, S.R., Toumi, R., Pfeifer, M., Turner, E.C., Nilus, R., Ewers, R.M., 2015. The relationship between leaf area index and microclimate in tropical forest and oil palm plantation: forest disturbance drives changes in microclimate. Agric. For. Meteorol. 201, 187–195.
Hirano, T., Jauhiainen, J., Inoue, T., Takahashi, H., 2009. Controls on the carbon balance of tropical peatlands. Ecosystems 12 (6), 873–887.
Hirano, T., Kusin, K., Limin, S., Osaki, M., 2014. Carbon dioxide emissions through oxidative peat decomposition on a burnt tropical peatland. Glob. Chang. Biol. 20 (2), 555–565.
Hirano, T., Segah, H., Harada, T., Limin, S., June, T., Hirata, R., Osaki, M., 2007. Carbon dioxide balance of a tropical peat swamp forest in Kalimantan, Indonesia. Glob. Chang. Biol. 13 (2), 412–425.
Hirano, T., Segah, H., Kitso, K., Limin, S., Takahashi, H., Osaki, M., 2012. Effects of disturbances on the carbon balance of tropical peat swamp forests. Glob. Chang. Biol. 18 (11), 3410–3422.
Husnain, H., Wigena, I.G.P., Dariah, A., Marwanto, S., Setyanto, P., Agus, F., 2014. CO_2 emissions from tropical drained peat in Sumatra, Indonesia. Mitig. Adapt. Strateg. Glob. Chang. 19 (6), 845–862.
IPCC, 2013. Climate Change 2013: The Physical Science Baisis. Cambridge University Press, Cambridge, United Kingdom, pp. 1535 pp.
Ishikura, K., Hirano, T., Okimoto, Y., Hirata, R., Kiew, F., Melling, L., Aeries, E.B., Lo, K.S., Musin, K.K., Waili, J.W., Wong, G.X, Ishii, Y., 2018. Soil carbon dioxide emissions due to oxidative peat decomposition in an oil palm plantation on tropical peat. Agric. Ecosyst. Environ. 254, 202–212.
Itoh, M., Okimoto, Y., Hirano, T., Kusin, K., 2017. Factors affecting oxidative peat decomposition due to land use in tropical peat swamp forests in Indonesia. Sci. Total Environ. 609, 906–915.
Iwata, H., Harazono, Y., Ueyama, M., Sakabe, A., Nagano, H., Kosugi, Y., Takahashi, K., Kim, Y., 2015. Methane exchange in a poorly-drained black spruce forest over permafrost observed using the eddy covariance technique. Agric. For. Meteorol. 214-215, 157–168.
Khasanah, N.m., van Noordwijk, M., Ningsih, H., Wich, S., 2015. Aboveground carbon stocks in oil palm plantations and the threshold for carbon-neutral vegetation conversion on mineral soils. Cogent Environ. Sci. 1, 1119964.
Kiew, F., Hirata, R., Hirano, T., Wong, G.X., Aeries, E.B., Musin, K.K., Waili, J.W., Lo, K.S., Shimizu, M., Melling, L., 2018. CO_2 balance of a secondary tropical peat swamp forest in Sarawak, Malaysia. Agric. For. Meteorol. 248, 494–501.
Kotowska, M.M., Leuschner, C., Triadiati, T., Meriem, S., Hertel, D., 2015. Quantifying above- and belowground biomass carbon loss with forest conversion in tropical lowlands of Sumatra (Indonesia). Glob. Chang. Biol. 21 (10), 3620–3634.
Luyssaert, S., Inglima, I., Jung, M., Richardson, A.D., Reichstein, M., Papale, D., Piao, S.L., Schulze, E.-.D., Wingate, L., Matteucci, G., Aragao, L., Aubinet, M., Beer, C., Bernhoffer, C., Black, K.G., Bonal, D., Bonnefond, J.-.M., Chambers, J., Ciais, P.,

Cook, B., Davis, K.J., Dolman, A.J., Gielen, B., Goulden, M., Grace, J., Granier, A., Grelle, A., Griffis, T., Grünwald, T., Guidolotti, G., Hanson, P.J., Harding, R., Hollinger, D.Y., Hutyra, L.R., Kolari, P., Kruijt, B., Kutsch, W., Lagergren, F., Laurila, T., Law, B.E., Le Maire, G., Lindroth, A., Loustau, D., Malhi, Y., Mateus, J., Migliavacca, M., Misson, L., Montagnani, L., Moncrieff, J., Moors, E., Munger, J.W., Nikinmaa, E., Ollinger, S.V., Pita, G., Rebmann, C., Roupsard, O., Saigusa, N., Sanz, M.J., Seufert, G., Sierra, C., Smith, M.-L., Tang, J., Valentini, R., Vesala, T., Janssens, I.A., 2007. CO_2 balance of boreal, temperate, and tropical forests derived from a global database. Glob. Chang. Biol. 13 (12), 2509–2537.

Malhi, Y., Pegoraro, E., Nobre, A.D., Pereira, M.G.P., Grace, J., Culf, A.D., Clement, R., 2002. The energy and water dynamics of a central Amazonian rain forest. J. Geophys. Res. 107 (D20), 8061. https://doi.org/10.1029/2001JD000623.

Manoli, G., Meijide, A., Huth, N., Knohl, A., Kosugi, Y., Burlando, P., Ghazoul, J., Fatichi, S., 2018. Ecohydrological changes after tropical forest conversion to oil palm. Environ. Res. Lett. 13 (6), 064035.

Marwanto, S., Agus, F., 2014. Is CO_2 flux from oil palm plantations on peatland controlled by soil moisture and/or soil and air temperatures? Mitig. Adapt. Strat. Glob. Chang. 19 (6), 809–819.

Massman, W.J., 2000. A simple method for estimating frequency response corrections for eddy covariance systems. Agric. For. Meteorol. 104, 185–198.

Meijide, A., Badu, C.S., Moyano, F., Tiralla, N., Gunawan, D., Knohl, A., 2018. Impact of forest conversion to oil palm and rubber plantations on microclimate and the role of the 2015 ENSO event. Agric. For. Meteorol. 252, 208–219.

Meijide, A., de la Rua, C., Guilaume, T., Röll, A., Hassler, E., Stielger, C., Tjoa, A., June, T., Corre, M.D., Veldkamp, E., Knohl, A., 2020. Measured greenhouse gas budgets challenge emission savings from palm-oil biodiesel. Nat. Commun. 11 (1), 1089.

Meijide, A., Röll, A., Fan, Y., Herbst, M., Niu, F., Tiedemann, F., June, T., Rauf, A., Hölscher, D., Knohl, A., 2017. Controls of water and energy fluxes in oil palm plantations: environmental variables and oil palm age. Agric. For. Meteorol. 239, 71–85.

Melling, L., Hatano, R., Goh, K.J., 2005a. Methane fluxes from three ecosystems in tropical peatland of Sarawak, Malaysia. Soil Biol. Biochem. 37 (8), 1445–1453.

Melling, L., Hatano, R., Goh, K.J., 2005b. Soil CO_2 flux from three ecosystems in tropical peatland of Sarawak, Malaysia. Tellus B 57 (1), 1–11.

Melling, L., Tan, C.S.Y., Goh, K.J., Hatano, R., 2013. Soil microbial and root respirations from three ecosystems in tropical peatland of Sarawak, Malyasia. J. Oil Palm Res. 25 (1), 44–57.

Miettinen, J., Hooijer, A., Vernimmen, R., Liew, S.C., Page, S.E., 2017. From carbon sink to carbon source: extensive peat oxidation in insular Southeast Asia since 1990. Environ. Res. Lett. 12 (2), 024014.

Miettinen, J., Shi, C., Liew, S.C., 2012. Two decades of destruction in Southeast Asia's peat swamp forests. Front. Ecol. Environ. 10 (3), 124–128.

Miettinen, J., Shi, C., Liew, S.C., 2016. Land cover distribution in the peatlands of Peninsular Malaysia, Sumatra and Borneo in 2015 with changes since 1990. Glob. Ecol. Conser. 6, 67–78.

Murdiyarso, D., Adiningsih, E.S., 2007. Climate anomalies, Indonesian vegetation fires and terrestrial carbon emissions. Mitig. Adapt. Strateg. Glob. Chang. 12 (1), 101–112.

Murdiyarso, D., Hergoualc'h, K., Verchot, L.V., 2010. Opportunities for reducing greenhouse gas emissions in tropical peatlands. Proc. Natl. Acad. Sci. 107 (46), 19655–19660.

Muscolo, A., Bagnato, S., Sidari, M., Mercurio, R., 2014. A review of the roles of forest canopy gaps. J. For. Res. 25 (4), 725–736.

Page, S.E., Rieley, J.O., Banks, C.J., 2011. Global and regional importance of the tropical peatland carbon pool. Glob. Chang. Biol. 17 (2), 798–818.

Papale, D., Reichstein, M., Aubinet, M., Canfora, E., Bernhofer, C., Kutsch, W., Longdoz, B., Rambal, S., Valentini, R., Vesala, T., Yakir, D., 2006. Towards a standardized processing of Net Ecosystem Exchange measured with eddy covariance technique: algorithms and uncertainty estimation. Biogeosciences 3, 571–583.

Reichstein, M., Falge, E., Baldocchi, D., Papale, D., Aubinet, M., Berbiger, P., Bernhofer, C., Buchmann, N., Gilmanov, T., Granier, A., Grünwald, T., Havránková, K., Ilvesniemi, H., Janous, D., Knohl, A., Laurila, T., Lohila, A., Loustau, D., Matteucci, G., Meyers, T., Miglietta, F., Ourcival, J.-.M., Pumpanen, J., Rambal, S., Rotenberg, E., Sanz, M., Tenhunen, J., Seufert, G., Vaccari, F., Vesala, T., Yakir, D., Valentini, R., 2005. On the separation of net ecosystem exchange into assimilation and ecosystem respiration: review and improved algorithm. Glob. Chang. Biol. 11 (9), 1424–1439.

Sakabe, A., Itoh, M., Hirano, T., Kusin, K., 2018. Ecosystem-scale methane flux in tropical peat swamp forest in Indonesia. Glob. Chang. Biol. 24 (11), 5123–5136.

Sakata, R., Shimada, S., Arai, H., Yoshioka, N., Yoshioka, R., Aoki, H., Kimoto, N., Sakamoto, A., Melling, L., Inubushi, K., 2015. Effect of soil types and nitrogen fertilizer on nitrous oxide and carbon dioxide emissions in oil palm plantations. Soil Sci. Plant Nutr. 61 (1), 48–60.

Sun, L., Song, C., Lafleur, P.M., Miao, Y., Wang, X., Gong, C., Qiao, T., Yu, X., Tan, W., 2018. Wetland-atmosphere methane exchange in Northeast China: a comparison of permafrost peatland and freshwater wetlands. Agric. For. Meteorol. 249, 239–249.

Thornley, J.H.M., 1976. Mathematical Models in Plant Physiology: a Quantitative Approach to Problems in Plant and Crop Physiology. Academic Press, pp. 318 pp.

Ueyama, M., Hirata, R., Mano, M., Hamotani, K., Harazono, Y., Hirano, T., Miyata, A., Takagi, K., Takahashi, Y., 2012. Influences of various calculation options on heat, water and carbon fluxes determined by open- and closed-path eddy covariance methods. Tellus B 64, 19048. https://doi.org/10.3402/tellusb.v64i0.19048.

Ueyama, M., Iwata, H., Harazono, Y., 2014. Autumn warming reduces the CO_2 sink of a black spruce forest in interior Alaska based on a nine-year eddy covariance measurement. Glob. Chang. Biol. 20 (4), 1161–1173.

Vickers, D., Mahrt, L., 1997. Quality control and flux sampling probelms for tower and aircraft data. J. Atmos. Oceanic Technol. 14, 512–526.

Wakhid, N., Hirano, T., Okimoto, Y., Nurzakiah, S., Nursyamsi, D., 2017. Soil carbon dioxide emissions from a rubber plantation on tropical peat. Sci. Total Environ. 581, 857–865.

Webb, E.K., Pearman, G.I., Leuning, R., 1980. Correction of flux measurements for density effects due to heat and water vapor transfer. Q. J. R. Meteorolog. Soc. 106, 85–106.

Wilczak, J.M., Oncley, S.P., Stage, S.A., 2001. Sonic anemometer tilt correction algorithms. Boundary Layer Meteorol. 106, 85–106.

Wong, G.X., Hirata, R., Hirano, T., Kiew, F., Aeries, E.B., Musin, K.K., Waili, J.W., Lo, K.S., Melling, L., 2020. How do land use practices affect methane emissions from tropical peat ecosystems? Agric. For. Meteorol. 282-283, 107869.

Yan, W., 2017. A makeover for the world's most hated crop. Nature 543 (16), 306–308.